Eur. Phys. J. D **20**, 243–249 (2002)
DOI: 10.1140/epjd/e2002-00117-0

THE EUROPEAN PHYSICAL JOURNAL D

Stacking faults in close-packed clusters

K. Manninen and M. Manninen[a]

Department of Physics, University of Jyväskylä, 40351 Jyväskylä, Finland

Received 6 February 2002 / Received in final form 11 April 2002
Published online 19 July 2002 –

Abstract. Ground state geometries of small hard sphere clusters were studied using two different type of contact interaction, a pair-potential and a many-atom interaction. Monte Carlo method in an FCC lattice with all possible (111) stacking faults was used to obtain the minimum energy geometries for clusters up to 59 atoms. Due to the surface energy, FCC packing is generally favoured as opposite to the HCP structure. However, in most cluster sizes the ground state obtained with the many-atom interaction has one or more stacking faults. The most symmetric geometry is usually not the ground state. Clusters with 59 and 100 atoms were studied due the possibility of a high symmetry cluster with stacking faults in all four directions. The size dependence of the total energy has similarities with that of the average moment of inertia.

PACS. 36.40.-c Atomic and molecular clusters – 61.46.+w Nanoscale materials: clusters, nanoparticles, nanotubes, and nanocrystals – 61.72.Nn Stacking faults and other planar or extended defects

1 Introduction

The ground state atomic arrangement, or geometry, determines many properties of small atomic clusters (for reviews see Refs. [1,2]). For instance stabilities, ionisation potentials and electronic properties in general [3,4] vibrational spectra, polarisabilities and thermal properties [5] of clusters are sensitive to the atomic arrangement in the cluster. Atoms which are bound together with pair-potential, like rare gases, or by metallic bonding tend to form close-packed structures, manifested by icosahedral or face-centered cubic structures. Rare gases as well as many metals (*e.g.* Na, Mg, Cu) show magic numbers corresponding to icosahedral packing [1,6] while others, like Al show magic numbers compatible by octahedral FCC packing [7]. The experimental results of free clusters at low temperatures usually suggest that the cluster is in its ground state geometry [1,8]. How the equilibrium is reached is an interesting research topic as such, including complicated diffusion mechanisms [9,10]. In this paper, however, we are not interested how the ground state is reached but what is its geometry and what is the role of stacking faults in the stabilisation of the geometry.

In the case of large clusters the optimal geometry is determined by the Wulff construction [11]. Molecular dynamics simulations have shown that the Wulff construction dominates only when the cluster has hundreds or thousands of atoms [9,12]. Due to the balance between the internal stress and the surface energy the geometry can depend on the size. For example, molecular dynamics simulations suggest that the best structures of nickel is icosahedron for $N < 2\,300$, decahedron for $2\,300 < N < 17\,000$ and an FCC polyhedron for $N > 17\,000$ [13].

In the case of small clusters with less than 100 atoms, most of the atoms are at the surface and the detailed surface geometry becomes important, while extended structural defects like stacking faults will have a small formation energy due to the finite size. This allows a huge number different isomers within a small energy range. Moreover, in simple metals the electronic structure with discrete energy levels plays an important role in determining the geometry [3,14]. The large number of isomers makes an *ab initio* determination of the cluster geometries difficult and consequently it is restricted to selected small sizes [15–20].

Systematic study of geometries of small clusters have been done by using model potentials, either pair-potentials or many-atom potentials, usually with parameters fitted to some experimental properties. Lennard-Jones (LJ) pair-potential has been most extensively used to study the ground states and low energy isomers. Doye *et al.* [21–23] used the LJ potential to determine a double-funnel energy landscape of the 38-atom cluster and to characterize the potential energy surfaces of clusters containing 13, 19, 31, 38, 55, 75, and 98 atoms. Doye and Wales [24] have used the modified Dzugutov potential to study the structures of polytetrahedral clusters. They found out magic numbers $N = 13$, 19, 23, 26, 29, 32, 34, 38, 42, 46, 57. Doye *et al.* have also used the potential of Pacheco and Prates-Ramalho up to $N = 105$ and found that found that the magic numbers ($N = 13$, 31, 33, 35, 38, 48, 50, 59) above

[a] e-mail: matti.manninen@phys.jyu.fi

the smallest 13 atom icosahedron are based on decahedral or close-packed structures. They used also the spherically averaged Girifalco potential, which gave magic numbers $N = 13$, 26, 29, 31, 33, 35, 38, 50, 57, 59 [25].

The aim of this paper is to study the effect of stacking faults in determining the ground state geometry of close-packed clusters. They are formed usually when atoms are bonded by a van der Waals interaction or by metallic bonding. A realistic model for rare gases would be the Lennard-Jones interaction and for metals any of the large number of many-atom interactions suggested in the literature [26]. Baskes [27] has studied the dependence of the lattice structure of the bulk metal of the parameters of the many-atom potential. The use of these kind of potentials would be important in studying the interplay between cubic and icosahedral structures, in a similar fashion as Doye and Wales [28] have done in the case of pair-wise interactions. However, we restrict to models which prevent formation of icosahedral and decahedral structures. Our goal is to understand general trends rather than study clusters of any specific material.

To this end we choose to use hard spheres. They allow only FCC and HCP lattice structures as well as their mixtures. We use two different models: a pair-wise contact interaction and a many-atom model, where the interaction energy is proportional to the square root of the coordination number. In large clusters the FCC structure dominates due to the fact that the low energy (111)-surface can have four different directions while in HCP it can have only one direction. This makes the Wulff construction of FCC to be energetically favourable as compared to that of HCP (note that in the hard sphere model the bulk energy is the same for FCC and HCP). In real clusters with long-range interactions, one has to take into account the strain energy, and the energy minimum is obtained as a balance between the coordination number and strain energy [23]. However, we use a contact interaction and the strain energy vanishes.

In this work we focus on the structure of clusters with ($N = 1...59$ and $N = 100$). In the size-range $N = 1...59$ most of the ground state clusters have stacking faults if the total energy is determined by a many-atom potential while a pair-potential typically produces many isomers with the same energy and, in most cases, at least one of them is a clean FCC cluster. Our results for the pair interaction are in agreement with those obtained by Doye and Wales [29] except for four sizes 33, 49, 50, and 51 for which we found a better ground state geometries.

We study the shape and the compactness of the cluster by determining the moments of inertia and show that the size-dependence of the total energy correlates with the size-dependence of the average momentum of inertia.

2 Optimization methods

We focus on a topological model for clusters. To this end we consider hard spheres with two different models for the contact interaction. In the pair-potential model (PP) the total energy is

$$E_{\mathrm{PP}} = -\frac{V}{2}\sum_{i}^{N} C_i \tag{1}$$

where C_i is the coordination number of the atom i and V is the strength of the interaction (V determines the energy scale). The second model (TB model) has a square root dependence of the coordination number

$$E_{\mathrm{TB}} = -\frac{V}{2}\sum_{i}^{N} \sqrt{C_i}. \tag{2}$$

The square root dependence can be derived from a simple tight-binding model [30,31] and has shown to be a good approximation for the tight binding model of small clusters [32]. Any nearest neighbour interaction gives the same cohesion energy for bulk FCC and HCP lattices, since the formation energy of stacking faults of (111)-layers has zero energy. In the case of a cluster all atoms do not have the same coordination and the optimal geometries of the two models can be different. Keeping the total coordination of the cluster fixed, the TB model favours structures where each atom have similar coordination while the PP model does not care how the bonds are distributed. We want to stress that although the square root approximation of equation (2) is quite accurate approximation for the true tight binding energy of surfaces, bulk defects and also for clusters, it does not take into account the discrete electron states which are important in small clusters. Consequently, the geometries obtained here for the small clusters using equation (2) should not be confused with the ground state geometries determined with the true tight binding method applied to hard spheres [33].

We first consider a pure FCC lattice. The atoms can only occupy fixed lattice sites. Finding the optimal geometry is then a straightforward optimization problem and a simple Monte Carlo procedure can be used to find the ground state geometry [34]. First an FCC lattice is generated inside a spherical volume and the lattice sites are randomly populated with N atoms. Next, the Metropolis algorithm is used to move atoms: an atomic configuration A_{i} is updated to A_{f} by selecting one of the atoms randomly and moving it to a randomly selected empty lattice site. The energy difference $\Delta E = E(A_{\mathrm{f}}) - E(A_{\mathrm{i}})$ determines whether the move is accepted ($\mathrm{e}^{-\Delta E/k_{\mathrm{B}}T} > \gamma$) or rejected ($\mathrm{e}^{-\Delta E/k_{\mathrm{B}}T} < \gamma$, where γ is a random number between 0 and 1). The simulation is started at a high temperature which is gradually decreased to zero. The optimization is repeated numerous times for each cluster size to obtain the ground state. Note that for many cluster the ground state is degenerate in the sense that there can be more than one topologically different cluster with the same energy, especially in the case of the pair-wise potential (the simplest example is the six-atom cluster which can be a perfect FCC octahedron or the five-atom geometry with one atom added, see Fig. 1. Both have 12 bonds.).

The possibility of stacking faults makes the procedure more complicated. We allow stacking faults in all four

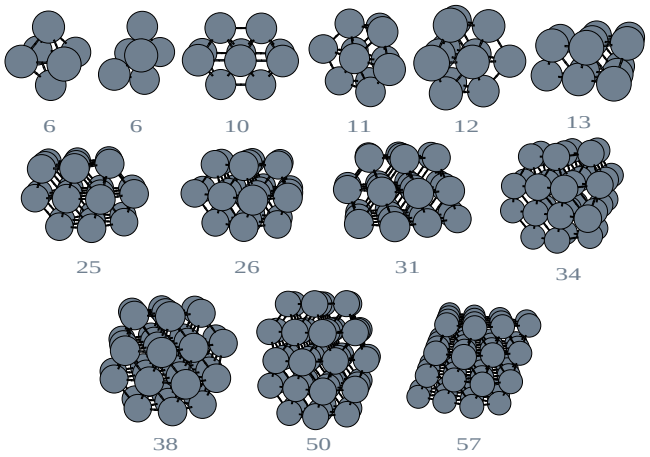

Fig. 1. A selection of the ground state geometries in the TB model. For the 6 atom cluster also the geometry based on the 5 atom bipyramid is shown. The sizes 11, 12, 26, 34, and 50 do not have FCC symmetry.

possible (111) directions and build a lattice including all possible sites generated by the stacking faults. In placing atoms in the lattice, we require that the minimum distance between any atom pair is the nearest neighbour distance in an FCC lattice (twice the hard sphere radius). The Monte Carlo simulation in this extended lattice becomes much slower than simulation in the pure FCC lattice. Moreover, due to the larger number of low-energy isomers more simulations are needed to find the ground state structure. Typically 500 to 1 000 simulations were done for each cluster size. For a given cluster size, several simulations ended to the same geometry. To identify the topology of the obtained cluster we determined both the radial and the angular distributions of the atoms.

For each cluster we determined the lowest energy isomers using both model potentials. In addition we determined the three moments of inertia for the principal axis and looked for correlation between the overall cluster shape and the ground state energy.

3 Results

Tables 1 and 2 give the lowest ground state energies found with the PP, equation (1), and the TB interaction, equation (2). For each size we show the energy of the best FCC geometry and the energy of the best geometry with one or more stacking faults (SF). In the cases of 4, 38, 39, and 40 atoms the cluster with stacking faults has always less bonds than the best FCC geometry. In those cases we have not determined the best SF geometry. The tables show that in most cases a SF structure has the same or lower energy than the best FCC geometry. Figures 1 and 2 show examples of the obtained ground state geometries of the TB model. Our ground state energies for the PP model agree with those of Doye and Wales [29] except for sizes 33, 49, 50, and 51 where we have found a better geometry (for 33, 49, 51 our results have one bond, for 50 two bonds more than those of Doye and Wales).

Table 1. The lowest energies of the FCC structures and structures with stacking faults (SF). N is the number of atoms. For the pair-potential model (PP) the (negative) energy is given as a number of bonds. For the many-atom model (TB) the total energy is given. The column "layers" give the numbers of atoms in each close-packed layer for the best FCC structure of the TB model. For $N = 4$, 38, 39, and 40 there is no SF structure with the same number or less bonds than in the best FCC structure.

N	$-E_{\mathrm{PP}}^{\mathrm{FCC}}$	$-E_{\mathrm{PP}}^{\mathrm{SF}}$	layers	$E_{\mathrm{TB}}^{\mathrm{FCC}}$	$E_{\mathrm{TB}}^{\mathrm{SF}}$
4	6		(3, 1)	−3.464	
5	8	9	(4, 1)	−4.439	−4.732
6	12	12	(3, 3)	−6.000	−5.968
7	15	15	(4, 3)	−7.220	−7.180
8	18	18	(5, 3)	−8.429	−8.434
9	21	21	(5, 4)	−9.650	−9.650
10	25	25	(5, 5)	−11.118	−11.100
11	28	29	(6, 5)	−12.327	−12.531
12	32	33	(7, 5)	−13.745	−13.950
13	36	36	(7, 6)	−15.177	−15.148
14	40	40	(4, 7, 3)	−16.575	−16.575
15	44	44	(4, 7, 4)	−18.002	−18.000
16	48	48	(6, 7, 3)	−19.403	−19.420
17	52	52	(6, 7, 4)	−20.813	−20.822
18	56	56	(6, 7, 5)	−22.214	−22.232
19	60	60	(7, 8, 4)	−23.643	−23.642
20	64	64	(7, 8, 5)	−25.053	−25.053
21	68	68	(8, 8, 5)	−26.453	−26.460
22	72	72	(8, 8, 6)	−27.852	−27.861
23	76	76	(7, 10, 6)	−29.262	−29.267
24	81	81	(7, 10, 7)	−30.869	−30.847
25	85	85	(8, 10, 7)	−32.270	−32.270
26	89	90	(9, 10, 7)	−33.671	−33.843
27	93	94	(9, 10, 8)	−35.064	−35.254
28	97	98	(8, 12, 8)	−36.471	−36.671
29	102	102	(10, 12, 7)	−38.070	−38.073
30	106	106	(11, 12, 7)	−39.471	−39.477
31	111	111	(12, 12, 7)	−41.070	−41.065
32	115	115	(12, 12, 8)	−42.462	−42.458
33	119	120	(12, 12, 9)	−43.855	−44.045
34	124	124	(9, 12, 9, 4)	−45.434	−45.441
35	128	129	(7, 12, 11, 5)	−46.816	−47.045
36	133	133	(7, 12, 12, 5)	−48.410	−48.437
37	138	138	(7, 12, 11, 7)	−49.996	−50.003
38	144		(7, 12, 12, 7)	−51.786	
39	148		(8, 12, 12, 7)	−53.179	
40	152		(9, 12, 12, 7)	−54.571	

Many of the clusters consist of only parallel (111)-layers. We denote these structures by the numbers of atoms in the layers. For example, the 13 atom cuboctahedron can be denoted as (3, 7, 3) FCC. The structures with stacking faults are denoted by SF or HCP. Note that all SF clusters can not be described with parallel (111) planes.

Table 2. The lowest energies of the FCC structures and structures with stacking faults (SF). N is the number of atoms. For the pair-potential model (PP) the (negative) energy is given as a number of bonds. For the many-atom model (TB) the total energy is given. The column "layers" give the numbers of atoms in each close-packed layer for the best FCC structure of the TB model.

N	$-E_{\rm PP}^{\rm FCC}$	$-E_{\rm PP}^{\rm SF}$	layers	$E_{\rm TB}^{\rm FCC}$	$E_{\rm TB}^{\rm SF}$
41	156	156	(8, 14, 12, 7)	−55.961	−55.974
42	160	160	(8, 14, 13, 7)	−57.360	−57.371
43	165	165	(8, 14, 13, 8)	−58.961	−58.972
44	169	169	(11, 14, 12, 7)	−60.350	−60.365
45	174	174	(10, 14, 13, 8)	−61.953	−61.954
46	178	178	(11, 14, 13, 8)	−63.345	−63.346
47	183	183	(12, 14, 13, 8)	−64.935	−64.933
48	187	187	(10, 16, 14, 8)	−66.308	−66.342
49	191	192	(10, 16, 14, 9)	−67.687	−67.933
50	196	198	(10, 16, 16, 8)	−69.282	−69.663
51	201	202	(10, 16, 15, 10)	−70.861	−71.056
52	207	207	(10, 16, 16, 10)	−72.651	−72.638
53	211	211	(11, 16, 16, 10)	−74.044	−74.021
54	216	216	(12, 16, 16, 10)	−75.635	−75.625
55	220	220	(12, 16, 16, 11)	−77.027	−77.018
56	225	225	(12, 16, 16, 12)	−78.617	−78.608
57	229	229	(13, 16, 16, 12)	−80.010	−79.980
58	233	234	(13, 19, 16, 10)	−81.360	−81.587
59	238	240	(10, 16, 16, 11, 6)	−82.949	−83.227
100	436	438	(18, 23, 24, 21, 14)	−146.368	−146.614

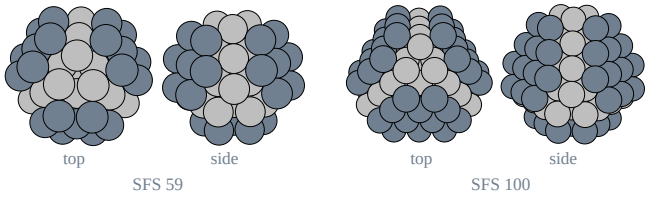

Fig. 2. The high-symmetry geometries of the 59 and 100 atom clusters. The dark spheres show the stacking fault layers at the surfaces. In both cases the FCC core is a truncated tetrahedron.

3.1 Size range N $\leq$ 13

For the smallest sizes there is not always a distinction between the FCC and HCP structure, for example, when the cluster consists of only two (111)-layers. Up to $N = 5$ there is only one clear ground state geometry. The five atom cluster is a trigonal bipyramid (tetrahedron with one atom on one of the triangular surface). This is the first clear HCP cluster. The six atom cluster shown in Figure 1 is the first one with two equally good geometries in the PP model, *i.e.* an octahedron and a five atom cluster with one atom added at any of the facets. In the TB model the octahedron is the ground state due to the fact that all the atoms have the same coordination. Similarly the cluster with seven atoms has two ground state isomers in the PP model: One atom is added on either of the six

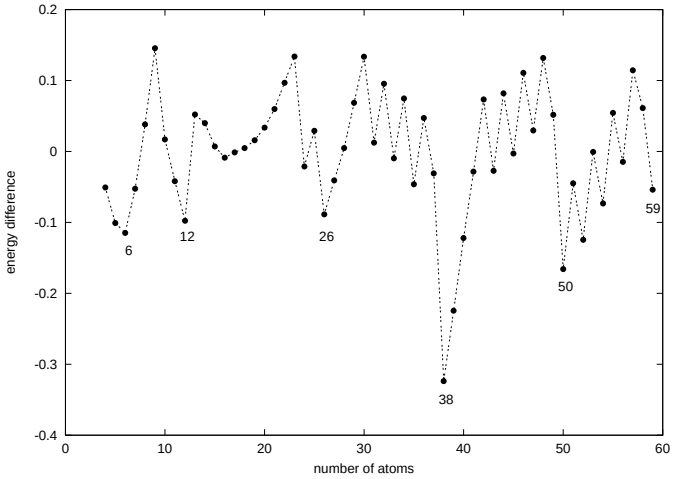

Fig. 3. The deviation of the ground state energy of the TB model from that calculated from the mass formula, equation (3). The numbers indicate the most stable sizes. The geometries of these are shown in Figures 1 and 2.

atomic clusters. In the TB model again the octahedral based FCC geometry is better.

For $N = 8$ the FCC structure is obtained by adding two atoms to the octahedron. An other structure with the same energy in the PP model is again obtained by adding an atom in the trigonal bipyramid-based $N = 7$ cluster. In this case the latter is the ground state of the TB model.

The cluster with more that 8 atoms have usually several different geometries with the same coordination number and consequently the same energy in the PP model. Especially, there are many isomers with stacking faults. In the TB model the nonlinearity of the energy on the local coordination reduces drastically the number of degenerate geometries. In the 9 and 10 atom cluster the best FCC and SF clusters still have the same energy in the PP model. For $N = 11$ and 12 the clusters with stacking faults are favourable in both models.

The cluster with 13 atoms is an interesting case. It has a compact high-symmetry FCC structure, a cuboctahedron, which is often considered to be a low energy configuration. However, there are two other geometries with the same coordination number, a cuboctahedron changed to an HCP cluster by rotating one of the surface triangles, and a two-layer structure shown in Figure 1. Surprisingly, the two-layer structure is the lowest energy state in the TB model. Note also that according to Figure 3 the size 13 is not magic in the hard sphere model.

3.2 Size range 14 $\leq$ N $\leq$ 19

In this size range there are three different domains of structures. The fcc structures are based on cuboctahedron and they have the lowest energy for $N = 14$ and 15. They are obtained by adding an atom on the square facet of the cuboctahedron. It is interesting to note that in the TB model the 15th atom should be placed on the opposite site than the 14th atom to minimize the energy.

This is actually the ground state geometry found for Al_{15} by Akola *et al.* [8]. For the 14 atom cluster the change of the cuboctahedron to HCP does not change the energy. In the PP picture the exists still another 14 atom structure with the same energy. However, in the TB model this geometry which is based on the 12 atom cluster has slightly higher energy than the ground state.

For $N = 16$ the FCC cluster is obtained by filling three of the six square facets on the cuboctahedron. It consists of three (111)-layers with 5, 7, and 3 atoms in each. We denote this structure (5, 7, 3) FCC. The TB energy is reduced by moving the third layer in the HCP site. The 17 atom cluster in TB model has two HCP geometries with the same energy, one with (5, 7, 5) structure and another with (5, 8, 4) structure. In the PP model these are degenerate with the best FCC geometry based on the cuboctahedron. In the 18 atom cluster the best TB geometry is based on the same HCP pattern (6, 8, 4).

The most symmetric geometry for 19 atoms is a perfect octahedron which has an FCC structure and high coordination. It consists of three (111)-layers with packing (6, 7, 6). However, there are several structures with the same PP energy, for example (7, 8, 4) FCC and (6, 7, 6) HCP, where one of the triangles of the octahedron is rotated, and also a packing (5, 9, 5). The lowest TB energy is obtained for two different geometries. One is an FCC geometry with (7, 8, 4) structure and the other a defected cluster, where the stacking faults destroy the simple layer structure. It is interesting to note that the TB energy of the most symmetric octahedral geometry is clearly above that of these two ground state structures.

3.3 Size range $20 \leq N \leq 40$

When the size is increased from 19 the clusters still consist mainly of only three (111)-layers. Size 20 is an exception having four layers (with a stacking fault). For most sizes the ground state TB geometry has one or more stacking faults. Sizes $N = 26$, 27, 28, 33, 35 have stacking faults also in the best PP structures. Consequently, in these cases the energy difference between the best FCC structures and the ground state is large also in the TB model.

In clusters with 38, 39, and 40 atoms there is only one kind of structure with a low PP energy, *i.e.* a truncated octahedron (38) with one or two atoms added. All geometries with stacking faults are much higher in energy. For 38 atoms the truncated octahedron is the ground state also for Lennard-Jones clusters [22] while in a realistic calculation for anionic Al_{38} resulted several less symmetric geometries with lower energies [34].

3.4 Size range $41 \leq N \leq 58$

In this size range the clusters consists mainly of four (111)-layers, three of the layers being in an FCC arrangement and the fourth layer in either FCC or HCP place. Cluster 46 is the first one showing stacking faults inside the cluster. This requires at least five parallel (111)-layers. It has a low-energy isomer (TB) with (5, 10, 12, 12, 7) structure where the first four layers form an HCP lattice and the three last an FCC lattice (ABABC packing), and a structure (7, 12, 12, 10, 5) structure where the first three and the last three layers have FCC packing, but the center layer is a stacking fault boundary (ABCBA packing).

The size 52 is the first having stacking faults in three different directions. Its core is a truncated tetrahedron with 31 atoms. Three of the facets have each a 7 atom hexagonal layer in a stacking fault position. The geometry is the same as in the 59 atom cluster shown in Figure 2, but the 7 atom hexagon is missing in one of the facets of the tetrahedron.

Coboctahedron is a high-symmetry geometry of a 55 atom cluster. However, like in the case of the 13 atom cluster the cuboctahedron is not the best FCC structure in the TB model. The best geometry has four (111)-layers (12, 16, 16, 11) instead of five layers (6, 12, 19, 12, 6) of the cuboctahedron. The Lennard-Jones pair-potential [21] as well as many-atom potential derived from the effective medium theory [35] give an icosahedral ground state. However, *ab initio* calculations for aluminium clusters suggest that the cuboctahedron is the ground state [36,34].

3.5 N = 59 and N = 100

The cluster with 59 atoms was the first one where a low energy geometry with stacking faults in all four directions was found. It consists of a truncated tetrahedron with additional SF layers on all four sites, as shown in Figure 2. The 100 atom cluster was studied due to the possibility of a similar geometry. Indeed this structure has a much lower total energy (both in PP and in TB models) than the best FCC geometry. The obtained SF geometry is most likely the ground state, although a complete search for the SF structures was not done in the case of $N = 100$.

3.6 Magic numbers

The total energy as a function of the cluster size reveals the most stable sizes. Often the second difference of the total energy is presented in looking for magic sizes. However, we will study the variation of the total energy per atom around a smooth curve fitted to the total energy values. This will show clearly not only the most stable sizes but also the regions of increased stability. The total energy is expressed as a "mass formula"

$$E_{\mathrm{ave}} = aN + bN^{2/3} + cN^{1/3}, \tag{3}$$

where the coefficients a, b, and c correspond to bulk cohesion energy, surface energy and curvature energy, respectively. We fix the coefficient a to the bulk value, which in the TB model is $a = -\sqrt{3}$ and obtain the best fit with $b = 1.158$ and $c = 0.375$.

Figure 3 shows the deviation of the energy per particle from the smooth function of equation (3). Sizes 12, 26, 38, 50, and 59 are clear minima showing enhanced stability

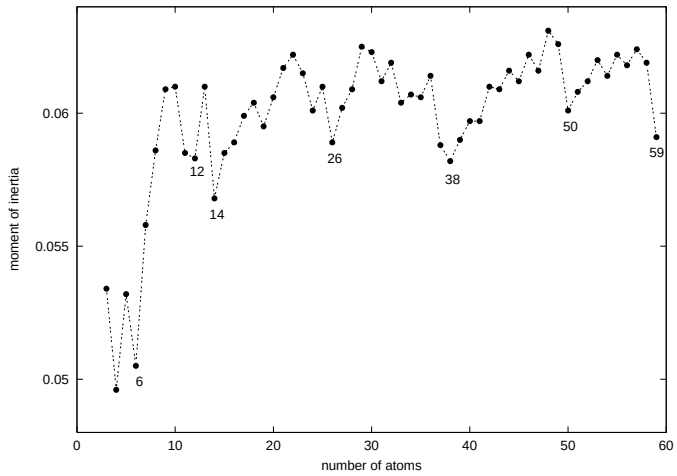

Fig. 4. The average moment of inertia, equation (4) as a function of the cluster size. Note that the minima at $N = 26$, 38, 50, and 59 coincide with the minima in the total energy shown in Figure 3.

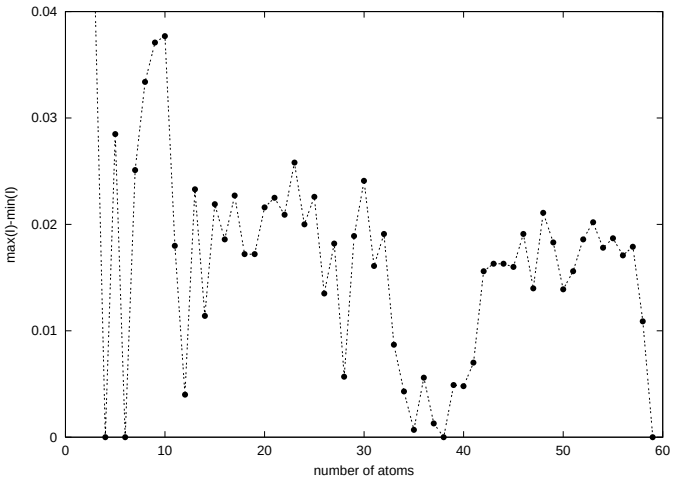

Fig. 5. The difference between the largest and the smallest components of the moments of inertia. When the difference is zero the cluster has a cubic symmetry.

(the geometries of these are shown in Figs. 1 and 2). Note that from these magic sizes only the 38 atom cluster is a pure FCC cluster, the others having stacking faults.

Doye and Wales [28] have used the pair-wise Morse potential to study the effect of the range of the potential on the magic numbers. For the hardest potential they also obtained the clusters with 26, 38, 50 and 59 to be "magic" in agreement with our results.

3.7 moments of inertia

The stability of the cluster is connected to the compactness of the cluster. The symmetry and relative size of the cluster can be determined with help of the moments of inertia. We have determined the three moments of inertia in the principal axis representation. For a spherical cluster the moment of inertia is proportional to $N^{5/3}$. We define a normalized moment of inertia as

$$I = \frac{1}{N^{5/3}} \sum_{i}^{N} (\mathbf{R}_i - \mathbf{R}_{\mathrm{cm}})^2, \qquad (4)$$

where $\mathbf{R}_i$ is the atom position and $\mathbf{R}_{\mathrm{cm}}$ the center of mass (in units of the FCC lattice constant). The normalized moment of inertia is shown in Figure 4. There is a striking similarity between Figures 3 and 4. The average moment of inertia, Figure 4, shows a marked minima at sizes 14, 26, 38, 50, and 59. All these except the size 14 are also minima in the total energy curve. Moreover, most of the fine details in the region from 26 to 59 are similar in Figures 3 and 4.

Figure 5 shows the difference between the maximum and minimum components of the moment of inertia in the principal axis representation. It reflects the symmetry of the cluster but is not necessarily an indication of a spherical shape (*e.g.* in a cubic symmetry all the components of are the same). It is interesting to note that in small sizes a more spherical shape does not necessarily mean smaller energy. For example, the cuboctahedron is not the smallest energy state of 13 atom cluster in the TB model. The "magic" 12 atom cluster has a rather high symmetry, as seen in Figure 5, but it is still much less symmetric than the (energetically less favourable) 14 atom cluster. Also the magic 26 and 50 atom clusters are strongly deformed from spherical (or cubic) symmetry.

4 Conclusion

We have studied the structures of hard sphere clusters with $N = 1...59$ and $N = 100$ as special case. We used a pair-potential and an many-atom interaction with a square root dependence of the coordination number. The total energy was minimized using a Monte Carlo method. For most sizes the pair-potential model resulted several isomers with the same total energy. Only for sizes $N < 5$ and $N = 38...40$. The FCC geometry was smaller in energy than any of the geometries with stacking faults. On the other hand, for $N = 5$, 11, 12, 26–28, 33, 35, 49–51, 58, 59, 100 the ground state of the pair-potential model does not have an FCC structure. Clusters with 59 and 100 atoms have a high symmetry and stacking faults on all surface facets.

The many-atom interaction is more sensitive in separating in energy the different isomers. In most cases it removes totally the degeneracy of the many ground state isomers of the pair-potential model and usually favours structures with stacking faults.

The energy as a function of the cluster size shows that sizes 12, 26, 38, 50, and 59 have strongest energy minima, but only the 38 atom cluster has a perfect FCC structure. The average moment of inertia correlates well with the total energy curve showing strong minima also at sizes 26, 38, 50, and 59. However, while these sizes are compact the variation of the components of the inertia tensor shows that the 26 and 50 atom clusters are still strongly deformed from the spherical (or cubic) symmetry.

We wish to thank A. Rytkönen and J. Akola for several valuable discussions. K.M. gratefully acknowledges a grant from the Väisälä foundation. This work has been supported by the Academy of Finland under the Finnish Centre of Excellence Programme 2000-2005 (Project No. 44875, Nuclear and Condensed Matter Programme at JYFL).

References

1. T.P. Martin, Phys. Rep. **273**, 199 (1996)
2. D.J. Wales, in *Atomic Clusters and Nanoparticles*, Les Houches Session LXXIII, edited by C. Guet, P. Hobza, F. Spiegelman, F. David (Springer, Heidelberg, 2001)
3. V. Bonačić-Koutecký, P. Fantucki, J. Koutecký, Chem. Rev. **91**, 1035 (1991)
4. J. Akola, K. Rytkönen, M. Manninen, Eur. Phys. J. D **16**, 21 (2001)
5. S. Kümmel, J. Akola, M. Manninen, Phys. Rev. Lett. **84**, 3827 (2000)
6. D. Reinhard, B.D. Hall, D. Ugarte, R. Monot, Phys. Rev. B **55**, 7868 (1997)
7. T.B. Martin, U. Näher, H. Schaber, Chem. Phys. Lett. **199**, 470 (1992)
8. J. Akola, M. Manninen, H. Häkkinen, U. Landman, Xi Li, L.-S. Wang, Phys. Rev. B **60**, 11297 (1999)
9. S. Valkealahti, M. Manninen, Phys. Rev. B **57**, 15533 (1998)
10. N. Combe, P. Jensen, A. Pimpinelli, Phys. Rev. Lett. **85**, 110 (2000)
11. A. Zangwill, *Physics at surfaces* (Cambridge University Press, 1988)
12. A.D. Bruce, A.N. Jackson, G.J. Ackland, N.B. Wilding, Phys. Rev. E **61**, 906 (2000)
13. C.L. Cleveland, U. Landman, J. Chem. Phys. **94**, 7376 (1991)
14. H. Häkkinen, J. Kolehmainen, M. Koskinen, P.O. Lipas, M. Manninen, Phys. Rev. Lett. **78**, 1034 (1997)
15. H. Häkkinen, M. Manninen, Phys. Rev. B **52**, 1540 (1995)
16. A. Rytkönen, M. Manninen, J. Chem. Phys. **113**, 4647 (2000)
17. V. Kumar, R. Car, Phys. Rev. B **44**, 8243 (1991)
18. P. Delaly, P. Ballone, J. Buttet, Phys. Rev. B **45**, 3838 (1992)
19. U. Röthlisberger, W. Andreoni, J. Chem. Phys. **94**, 8129 (1991)
20. J. Akola, H. Häkkinen, M. Manninen, Phys. Rev. B **58**, 3601 (1998)
21. J.P.K. Doye, M.A. Miller, D.J. Wales, J. Chem. Phys. **110**, 6896 (1999)
22. J.P.K. Doye, M.A. Miller, D.J. Wales, J. Chem. Phys. **111**, 8417 (1999)
23. R.H. Leary, J.P.K. Doye, Phys. Rev. E **60**, 6320 (1999)
24. J.P.K. Doye, D.J. Wales, Phys. Rev. Lett. **86**, 5719 (2001)
25. J.P.K. Doye, D.J. Wales, W. Branz, F. Calvo, Phys. Rev. B **64**, 235409 (2001)
26. *Many-Atom Interactions in Solids*, edited by R.M. Nieminen, M.J. Puska, M.J. Manninen (Springer, Heidelberg, 1990)
27. M.I. Baskes, Phys. Lev. Lett. **83**, 2592 (1999)
28. J.P.K. Doye, D.J. Wales, J. Chem. Soc. Faraday Trans. **93**, 4233 (1997)
29. J.P.K. Doye, D.J. Wales, Chem. Phys. Lett. **247**, 339 (1995)
30. R.P. Gupta, Phys. Rev. B **23**, 6265 (1981)
31. M.W. Finnis, J.E. Sinclair, Phil. Mag. A **50**, 45 (1984)
32. H. Häkkinen, J. Mansikka-Aho, M. Manninen, J. Phys. Cond. Matt. **3**, 7757 (1991)
33. A. Yoshida, T. Døssing, M. Manninen, J. Chem. Phys. **101**, 3041 (1994)
34. J. Akola, M. Manninen, H. Häkkinen, U. Landman, Xi Li, L.-S. Wang, Phys. Rev. B **62**, 13216 (2000)
35. S. Valkealahti, M. Manninen, Phys. Rev. B **45**, 9495 (1992)
36. Jae-Yel Yi, D.J. Oh, J. Bernholc, R. Car, Chem. Phys. Lett. **174**, 461 (1990)